

Projecting Rates of Spread for Invasive Species

Michael G. Neubert^{1*} and Ingrid M. Parker²

All else being equal, the faster an invading species spreads, the more dangerous its invasion. The projection of spread rate therefore ought to be a central part of the determination of invasion risk. Originally formulated in the 1970s to describe the spatial spread of advantageous alleles, integrodifference equation (IDE) models have since been co-opted by population biologists to describe the spread of populations. More recently, they have been modified to include population structure and environmental variability. We review how IDE models are formulated, how they are parameterized, and how they can be analyzed to project spread rates and the sensitivity of those rates to changes in model parameters. For illustrative purposes, we apply these models to *Cytisus scoparius*, a large shrub in the legume family that is considered a noxious invasive species in eastern and western North America, Chile, Australia, and New Zealand.

KEY WORDS: *Cytisus scoparius*; demography; integrodifference equations; invasion rates; matrix models; nonnative; spread

1. INTRODUCTION

The invasion of nonindigenous species is now considered to be one of the most serious problems facing native ecosystems,⁽¹⁾ and invaders have received increasing attention for their considerable economic and social impacts.^(2,3) National governments have responded with demands for more effective national and regional policies to combat the introduction and spread of harmful invaders.^(2,4) Such policies, however, are likely to come with significant costs. Regulations on interstate and international trade, quarantine and inspection services at state borders, and government-sponsored eradication programs are all examples of programs that could reduce the negative effects of introduced species, but will be costly. To be

justifiable, policy actions for exotic species should be based on explicit assessments of risks.^(5,6)

At the local level, managers of protected natural landscapes are faced every day with decisions about which invasive species to control with limited funds. Most nature reserves have significant problems caused by more than one, and sometimes many, problematic nonindigenous species.⁽⁷⁾ Often, decisions about which species to eradicate or control are made on an *ad hoc* basis, in part based on the total current acreage of a species and therefore its visibility. While this decision-making process can seem idiosyncratic, some attempts have been made to develop systematic procedures.⁽⁸⁾ Under the best circumstances, decisions on how to allocate resources to nonnative species management should be based on a risk analysis that evaluates the potential for long-term, negative effects on natural ecosystems, including populations of native species.

Such an analysis needs to consider several factors. First is the projected effect of the species over the whole protected landscape, which requires knowing the likelihood that a species will invade different

¹ Biology Department, MS 34, Woods Hole Oceanographic Institution, Woods Hole, MA 02543, USA.

² Department of Ecology and Evolutionary Biology, University of California at Santa Cruz, Santa Cruz, CA 95064, USA.

* Address correspondence to Michael G. Neubert, Biology Department, MS 34, Woods Hole Oceanographic Institution, Woods Hole, MA 02543, USA; mneubert@whoi.edu.

types of habitats. Second is the actual response of the ecosystem to the presence of sustained populations of the invader, which will be a function of the species' density as well as its per-capita effects.⁽⁹⁾ Introduced species can have effects at the individual level (e.g., by changing the behavior or size of native species), at the population level (e.g., by changing the abundance or extinction risk of native populations), at the community level (by affecting diversity or composition), and at the ecosystem level (by altering functions such as carbon storage or hydrology).

At least initially, the costs associated with each of these effects will grow with time as the invader occupies new habitat. If costs are proportional to the area occupied,⁽⁹⁾ these costs will grow at a rate proportional to the invasion rate—the rate at which the invader spreads through the habitat. Remediation and removal costs will also increase with the area occupied, and may increase with the amount of time a site has been invaded.⁽¹⁰⁾ Thus a projection of invasion rate is a crucial element of a cost-benefit analysis. The higher the projected invasion rate, the more quickly costs will accumulate, and the more expensive inaction becomes.

In this article, we describe the use of various population models for projecting the spread of an invasive species. We begin, in Section 2, with a brief review of the classic approach to the problem using Fisher's equation, and then summarize the shortcomings of this approach. We then describe the formulation of integrodifference equation (IDE) models for population growth and dispersal.^(11,12) Rather than jumping directly to the most general model, we will build from the simplest case and develop examples along the way. In Section 3.1, we construct scalar IDEs that, while treating all individuals as identical in their vital and dispersal rates, allow for a very flexible description of dispersal. We review how to calculate invasion rates for these models in Section 3.2. In Section 3.3, we describe how to incorporate dispersal data into IDE models, and investigate the effects of environmental variability in Section 3.4. In Section 3.5, we construct integrodifference matrix population (IMP) models that allow us to specify stage-specific vital rates and dispersal distributions. Finally, in Section 4, we end with a discussion of potential uses and misuses of our approach.

1.1. *Cytisus scoparius*

To illustrate the use of IDE and IMP models, we will apply them to the invasive plant *Cytisus scoparius*

(Scotch broom or broom). Broom is a large shrub in the legume family. Native to Europe and the British Isles, it has been introduced into many regions where it is considered a noxious invasive species, including eastern and western North America, Chile, Australia, and New Zealand.^(13–15) The economic importance of broom is tied to its aggressive invasion of pastures, reforested areas, and roadsides.^(13,16) Although a comprehensive study of its economic impact has not been done, over \$220,000 per year is spent to control broom along roadsides in the State of Oregon alone.⁽¹⁶⁾ Aside from economic factors, broom is also a conservation threat. Thick stands of broom have eliminated native herbs and tree seedlings in Australia⁽¹⁷⁾ and reduced native plant diversity in prairies of the Pacific Northwest.⁽¹⁸⁾ Ecosystem effects of broom include an increase in carbon and nitrogen pools and a dramatic increase in nitrogen availability.⁽¹⁹⁾

The population dynamics and dispersal of broom were studied in Washington State, USA, where the plant invades both anthropogenically disturbed urban fields and relatively undisturbed glacial outwash prairies.^(18,20) Broom has two dispersal mechanisms. First, pods dry out and burst, ballistically dispersing seeds. Second, seeds are attached to elaiosomes (lipid-rich bodies), which are attractive to ants. Ants carry seeds toward or into their nests, then remove the elaiosome and discard the seed.⁽²¹⁾ Strong density dependence results in significant variation in demographic rates from the edge to the center of a broom infestation.⁽²⁰⁾ Demographic rates also vary among sites; population growth is more rapid in prairies than urban fields. For this article, we will use demographic parameters estimated at the expanding edge of one urban population in Discovery Park, Seattle.⁽²⁰⁾

2. FISHER'S EQUATION

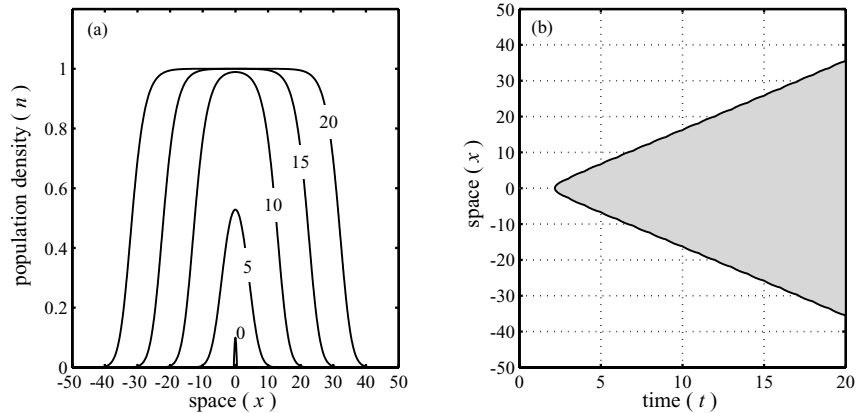
Perhaps the simplest model for the population growth and spread is a reaction-diffusion equation called "Fisher's equation":^(22–24)

$$\frac{\partial n}{\partial t} = rn \left(1 - \frac{n}{K}\right) + D \frac{\partial^2 n}{\partial x^2}. \quad (1)$$

Here, $n(x, t)$ represents the population density at location x and time t , r is the intrinsic rate of population increase, K is the environmental carrying capacity, and D is the diffusion coefficient. Fig. 1 shows a typical solution of Fisher's equation, and also illustrates how we define the rate of spread in a one-dimensional model.

We imagine there is some threshold population density below which we cannot detect the presence of

Fig. 1. A typical solution of Fisher’s equation exhibits the essential dynamic of an invasion: population growth and spread. For this simulation, we set $r = D = 1$. In (a) we plot the solution at $t = 0, 5, 10, 15, 20$. In (b), the gray area marks the region in space where the population size is larger than 0.1. The boundaries of this area have slopes equal to the rate of spread, $c = 2\sqrt{rD} = 2$.



the population. We call this threshold density \hat{n} , and we use $\hat{x}(t)$ for the location where the population density equals \hat{n} . The asymptotic rate of spread is defined as the rate of increase of $\hat{x}(t)$ as t becomes large:

$$c = \lim_{t \rightarrow \infty} \frac{d\hat{x}(t)}{dt}. \tag{2}$$

For Equation (1),

$$c = 2\sqrt{rD} \tag{3}$$

(see References 25 and 26).

Fisher’s equation has been used to study the rates of spread of a wide variety of invasive species.^(27,28) There are, however, a number of shortcomings with the model that make a different approach, which we describe in the next section, more appealing. The first shortcoming is that Fisher’s equation assumes diffusive movement; i.e., it assumes that the distribution of dispersal distances is normal. This is rarely true. In fact, there are a wide variety of measured distributions and many of these are leptokurtic,⁽²⁹⁾ being more peaked about their mode and having fatter tails than a normal distribution with the same variance. Second, it assumes that the individuals within the population are identical in both their vital rates and in their propensity for dispersal. Again, this is rarely true. Vital rates and dispersal rates are usually strongly determined by the stage of the individual within the life cycle. For example, seeds are dispersed and typically suffer high mortality rates, while mature plants do not disperse but have relatively low mortality rates.

IDE models address some of the shortcomings of Fisher’s equation. In the next sections we describe the formulation of these models.^(11,12) We build from relatively simple to more complex cases, using broom to illustrate each formulation.

3. INTEGRODIFFERENCE EQUATION MODELS

3.1. Scalar Models

We begin by considering a population of a single species composed of identical individuals distributed along an infinite one-dimensional habitat. We imagine that the change in population density from one time to the next is the result of two processes: population growth and dispersal. We assume that these processes act sequentially. First, population growth acts to change local population density via the function

$$n(y, t + 1) = f[n(y, t)]. \tag{4}$$

Then, dispersal acts to spatially redistribute individuals. If the probability of dispersing from location y to location x is given by the probability density function $k(x, y)$, then after dispersal the population density is given by the IDE⁽¹¹⁾

$$n(x, t + 1) = \int_{-\infty}^{\infty} k(x, y) f[n(y, t)] dy. \tag{5}$$

If, in addition, the probability of moving from point y to point x only depends upon the relative locations of the two points, then $k(x, y) = k(x - y)$, and Equation (5) becomes

$$n(x, t + 1) = \int_{-\infty}^{\infty} k(x - y) f[n(y, t)] dy. \tag{6}$$

Because the integral in Equation (6) is a convolution integral, this model is easier to analyze and to numerically simulate than Equation (5).⁽³⁰⁾

3.2. Rates of Spread

Solutions to the IDE Equation (6) on an infinite domain are often qualitatively similar to solutions to

the reaction-diffusion Equation (1). In fact, the rates of spread they generate can be made quantitatively equivalent⁽³¹⁾ by using a normal distribution for k , and a compensatory growth function for f . With the right parameters, we would then exactly duplicate Fig. 1b, using Equation (6).

As long as the population can grow when small (i.e., $\lambda = f'(0) > 1$) and increased density has a negative effect on vital rates (i.e., $\lambda n > f(n)$ for all n), then a population initially restricted to a finite portion of space grows and spreads under Equation (6). If, in addition, the dispersal kernel has a moment-generating function $M(s)$ defined by

$$M(s) = \int_{-\infty}^{\infty} k(x)e^{sx} dx, \quad (7)$$

then the solution eventually converges to a traveling wave⁽³²⁾ with constant speed. Weinberger^(33,34) showed that the eventual rate of spread (or invasion rate) is given by

$$c = \min_{s>0} \left\{ \frac{1}{s} \ln[\lambda M(s)] \right\}. \quad (8)$$

It should be noted that there are kernels without moment-generating functions. These kernels have fat tails (i.e., they are not exponentially bounded), and produce accelerating invasion rates. In most cases, the rate of acceleration cannot be computed analytically, but if the kernel has finite moments of all orders then Kot *et al.*⁽³¹⁾ showed how to approximate the rate of acceleration. For the remainder of our presentation here, we will assume that all dispersal kernels have exponentially bounded tails. All kernels that have a maximum potential dispersal distance fall into this category.

3.3. Dispersal Kernels

The principal advantage of the IDE Equation (6) over the reaction-diffusion Equation (1) is that a variety of dispersal distributions can be incorporated through the dispersal kernel $k(x, y)$.⁽³⁵⁾ In this section, we review how one might construct a dispersal kernel depending on the questions and data at hand.

3.3.1. Mechanistic Models

In many instances, while one may have very little data on the actual dispersal patterns of a given species in a given habitat, one may have a good idea about the mechanisms an organism uses for dispersal. Alternatively, one may be interested in the relative im-

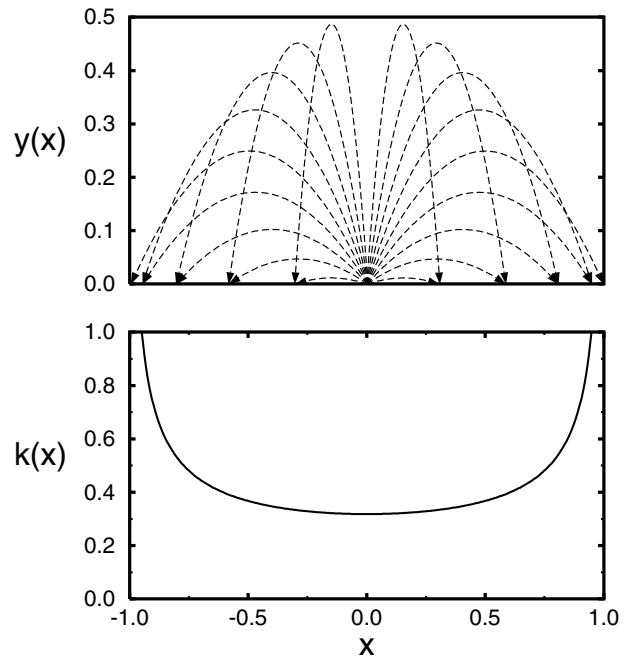


Fig. 2. Ballistic dispersal. The top graph shows the trajectories of propagules launched at various angles and moving under the influence of gravity. Although the angles are uniformly distributed, the landing sites cluster near the maximal dispersal distance. This produces a redistribution kernel (bottom panel and Equation (9)) with singularities at $x = \pm v^2/g$. In this figure, $v^2 = g$ (from Neubert *et al.*)⁽³⁵⁾

portance that a particular dispersal mechanism plays in the overall dispersal process. In the case of broom there are two principal dispersal mechanisms: ballistic dispersal and ant-mediated dispersal. (We do not consider human-mediated dispersal here, but discuss its relevance for the estimation of large-scale spread rates in Section 4.) Let us first consider these mechanisms separately.

Mechanistic models for ballistic dispersal can be quite complicated.⁽³⁶⁾ A simple, illustrative model is one in which propagules are launched at a random angle, but fixed speed v , in one spatial dimension (Fig. 2). The dispersal kernel that results from such a process is given by

$$k_b(x) = \frac{1}{\pi \sqrt{(v^2/g) - x^2}}, \quad (9)$$

where g is the acceleration due to gravity.⁽³⁵⁾

One can imagine that ants redistribute seeds in the following way. After an ant picks up a seed, it performs a diffusive random walk, with diffusion parameter D . In each (infinitesimally) small interval of

time Δt , the ant has a small probability of releasing the seed given by $h\Delta t$. Given these two processes, the probability that a seed starting at the origin moves to location x is given by the Laplace distribution⁽³⁷⁾

$$k_a(x) = \sqrt{\frac{h}{4D}} \exp\left[-|x|\sqrt{\frac{h}{D}}\right]. \quad (10)$$

This distribution is often used in theoretical studies of dispersal because it captures the leptokurtosis found in many observed dispersal distributions and lends itself to simple mathematical analyses.

Combining two dispersal processes (e.g., ballistic and ant dispersal) is relatively simple. As long as the two processes are independent, the combined dispersal kernel is formally given by the convolution of the two kernels k_b and k_a

$$k_c(x) = \int_{-\infty}^{\infty} k_a(x-y)k_b(y) dy. \quad (11)$$

In some cases, the convolution of Equation (11) is not given in terms of elementary functions. This is the case when we convolve the ballistic and ant-dispersal kernels of Equations (9) and (10) (Fig. 3). A convenient consequence of Equation (11) is that the moment-generating function for the combined kernel is simply the product of the moment-generating functions of the two kernels separately:

$$M_c(s) = M_a(s)M_b(s). \quad (12)$$

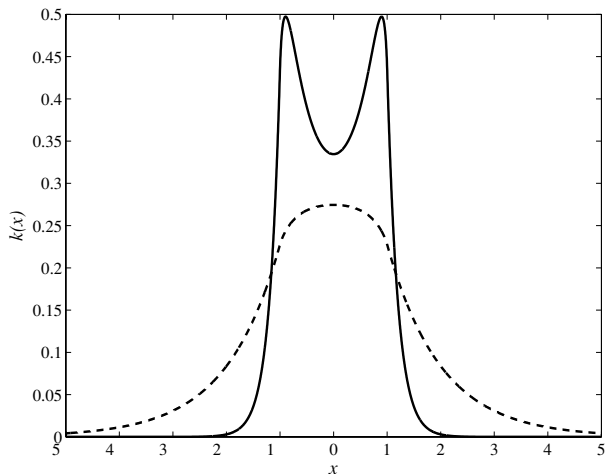


Fig. 3. Ballistic plus ant dispersal. As in Fig. 2, $v^2 = g$. When ant dispersal is large relative to ballistic dispersal, the kernel resulting from the combined action of ants and ballistic dispersal is unimodal (dashed curve, $\sqrt{h/D} = 1$). The kernel is bimodal if ant dispersal is relatively short range (solid curve, $\sqrt{h/D} = 5$).

Thus, if we are only interested in a projection of the speed (cf. Equation (8)), we need never actually compute the convolution of Equation (11).

3.3.2. Measured Distributions

If one is lucky enough to have measurements of dispersal distance, one can use them directly. This is perhaps the most appealing feature of IDE models. In the literature, these measurements are often reported as histograms of dispersal distance. Some care must be taken in translating these histograms into one-dimensional dispersal kernels, since the data are often collected in two spatial dimensions.³

Fig. 4A shows a two-dimensional histogram of ballistic seed dispersal distances collected for broom.⁽³⁹⁾ Rectangular strips $1\text{ m} \times 8\text{ m}$ were placed around isolated plants and coated with Tanglefoot glue to catch seeds. The number of seeds within each 0.5 m segment was adjusted by the proportion of the total area searched, to estimate the total number of seeds landing within the annulus at that distance. Converting these data into a bivariate probability density function, then taking the marginal distribution over any direction,⁽³⁸⁾ gives the one-dimensional dispersal kernel (Fig. 4B)

$$k_b(x) = \begin{cases} 2 \sum_{i=j}^m (g_i - g_{i+1}) \sqrt{x_i^2 - x^2}, & \text{if } x_{j-1} < |x| \leq x_j, j = 1, 2, \dots, m, \\ 0, & \text{otherwise,} \end{cases} \quad (13)$$

where $g_i = \phi_i/A_i$, A_i is the area of the annular region bounded by the radii x_{i-1} and x_i , and ϕ_i is the frequency of seeds in that annular region.

Secondary dispersal of broom seeds after their ballistic dispersal from the plant was quantified by measuring the distances to seedlings in the spring from points where seed piles were put out at the time of seed maturation in the fall.⁽³⁹⁾ These data are different from those used to form the kernel in Equation (13) in that they are a set of distances rather than frequencies in ranges. Assuming radial symmetry then gives a two-dimensional “histogram” as shown in Fig. 4C. In this figure, each cylinder, with radius r_i and height b_i , is a representation of the two-dimensional Dirac delta function⁽⁴⁰⁾ with intensity b_i , in polar coordinates: $b_i\delta_2(r - r_i)$. b_i is the number of seedlings found at

³ These issues are dealt with more thoroughly in Reference 38. We repeat some of that material here for the reader’s convenience.

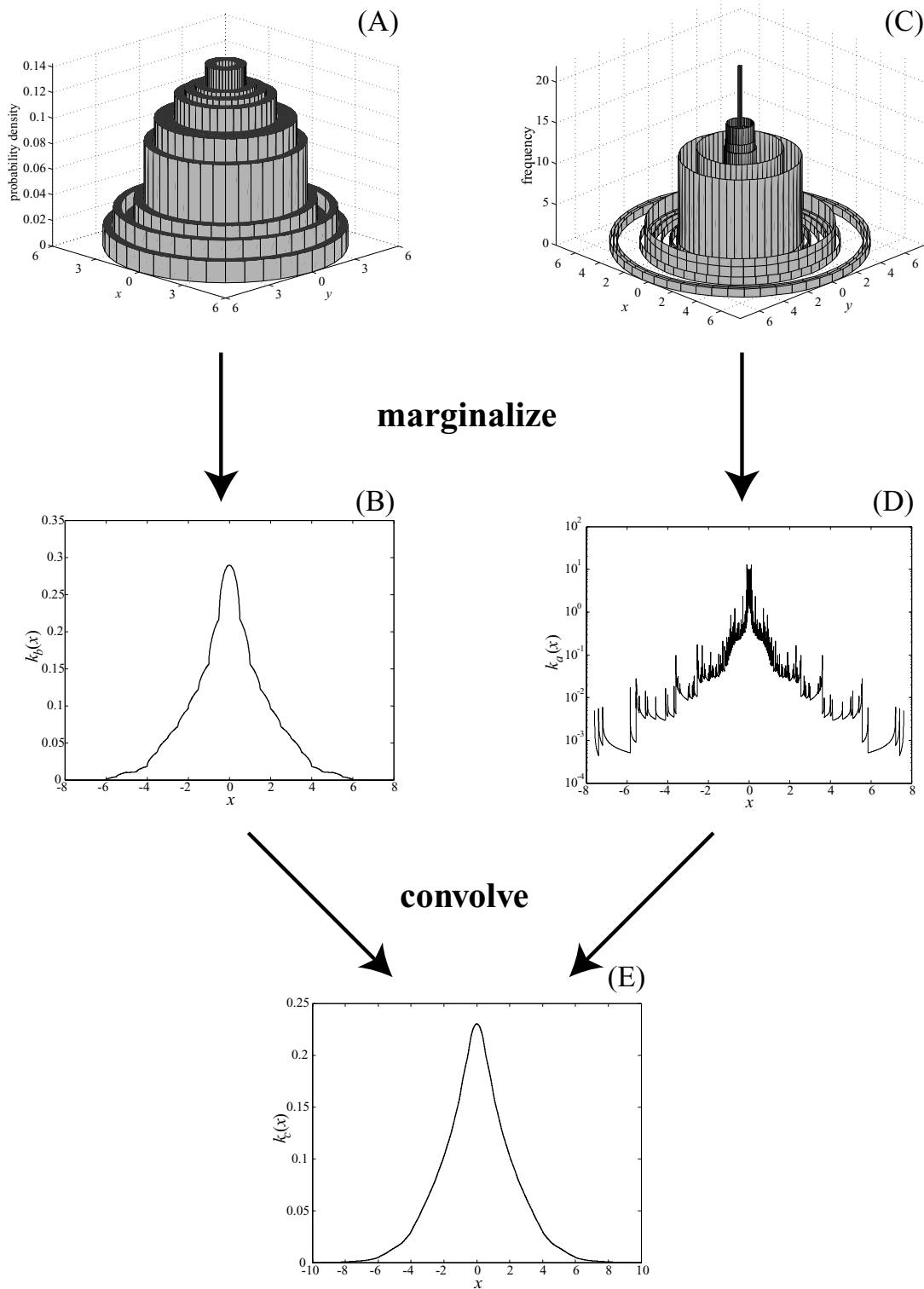


Fig. 4. Estimated dispersal kernels for broom. Two-dimensional histograms of dispersal distances were constructed from measurements⁽³⁹⁾ of ballistic dispersal (A) and ant dispersal (C). These were marginalized (i.e., integrated over one direction) to obtain one-dimensional dispersal kernels (B, D). The convolution of these one-dimensional kernels produces the composite dispersal kernel k_c (E).

that distance. Given ℓ seedlings, the marginal distribution in the x direction is then obtained by integrating over y yielding⁽³⁸⁾

$$k_a(x) = \sum_{i=1}^{\ell} h_i(x), \quad (14)$$

with

$$h_i(x) = \begin{cases} [\pi^2(r_i^2 - x^2)]^{-1/2}, & \text{if } |x| < r_i, \\ 0, & \text{otherwise.} \end{cases} \quad (15)$$

There is a convenient expression for the moment-generating function of k_a

$$M_a(s) = \frac{1}{\ell} \sum_{i=1}^{\ell} I_0(r_i s), \quad (16)$$

where I_0 is the modified Bessel function of the first kind.⁽⁴¹⁾ Equation (16) can be thought of as an unbiased nonparametric estimator for the moment-generating function of k_a .⁽⁴²⁾ We know of no simple expression for the moment-generating function for k_b ; it must be computed numerically.

If every seed is dispersed by an ant, then the composite dispersal kernel, taking into account both dispersal processes, is given by Equation (11) (Fig. 4E), and the moment-generating function for the composite kernel is given by Equation (12). Of course some seeds are never touched by an ant. If each seed has a probability p of being dispersed by an ant, then the composite kernel is given by

$$k_c(x; p) = \int_{-\infty}^{\infty} [pk_a(x - y) + (1 - p)\delta(x - y)]k_b(y) dy, \quad (17)$$

and the moment-generating function is given by

$$M_c(s) = [1 - p + pM_a(s)]M_b(s). \quad (18)$$

Using Equation (8) with Equation (18), along with the estimate of population growth rate for broom in Discovery Park during the 1993–1994 season⁽³⁹⁾ ($\lambda_{1993} = 1.2167$), we computed the invasion rate (c) as a function of the ant-dispersal probability (p). A graph of this function (Fig. 5) shows that invasion rate increases roughly linearly and by approximately 17% as the ant-dispersal probability increases from 0 to 1. As estimated by a field experiment,⁽³⁹⁾ ants dispersed approximately 90% of the seeds, resulting in an estimated invasion rate of 1.35 m/yr. We will set $p = 0.9$ in the examples that follow.

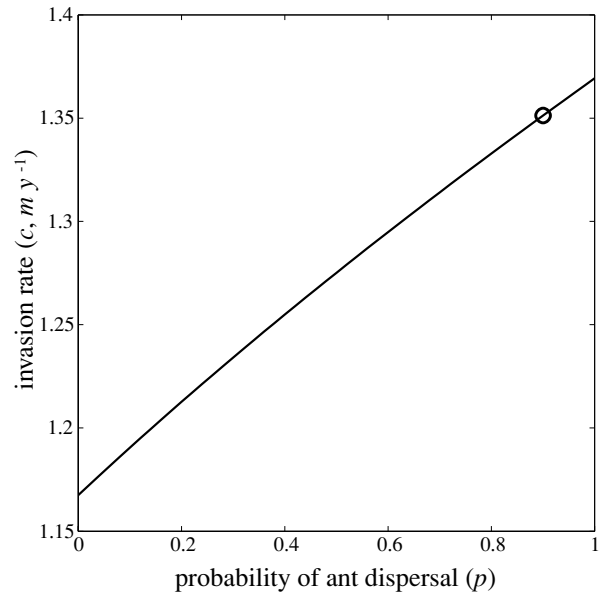


Fig. 5. Invasion rate (c) as a function of the probability of ant dispersal (p). Invasion rate was calculated using Equations (8) and (18), with the numerically estimated moment-generating functions for the estimated ballistic and ant-dispersal kernels (cf. Fig. 4). Population growth rate was taken to be $\lambda_{1993} = 1.2167$, as estimated for Discovery Park, Seattle, Washington.⁽²⁰⁾ The value of p estimated from the data (≈ 0.9) and the resulting speed (≈ 1.35 m/yr) are marked with a circle.

3.4. Periodic and Stochastic Environments

The models we have described so far assume a temporally homogeneous environment. In some cases, this assumption will be too far from the truth to be useful. In addition, one may be interested in how environmental variability affects invasion rates. Neubert *et al.*⁽⁴³⁾ show how to calculate time-averaged invasion rates in periodic environments, and expected time-averaged invasion rates in stochastic environments.

Environmental stochasticity can be incorporated into Equation (6) by choosing the growth rates and dispersal kernels at random from a set of choices. The model then becomes

$$\mathcal{N}(t + 1, x) = \int_{-\infty}^{\infty} \mathcal{K}_t(x - y) f(\mathcal{N}(t, y); \Lambda_t) dy, \quad (19)$$

where the $\mathcal{K}_t(x - y)$ are independent and identically distributed (i.i.d.) random dispersal kernels, and the growth rates Λ_t are i.i.d. random variables independent of the kernels. (The script \mathcal{N} is used to emphasize that population density is now a random function.)

At any time t , the population has a random extent \mathcal{X}_t , defined to be the location farthest from the invasion's origin with $\mathcal{N}(t, x) \geq \hat{n}$. The average speed since the invasion began is also a random variable, given by $\bar{C}_t = (\mathcal{X}_t - x_0)/t$. Neubert *et al.*⁽⁴³⁾ showed that \bar{C}_t is asymptotically normally distributed with mean (μ) and variance (σ^2) given by

$$\mu = \min_s E \left\{ \frac{\ln[\Lambda_0 M_0(s)]}{s} \right\}, \quad (20)$$

and

$$\sigma^2 = \frac{1}{t} \text{Var} \left\{ \frac{\ln[\Lambda_0 M_0(s^*)]}{s^*} \right\}, \quad (21)$$

where s^* is the value of s that gives the minimum for μ . As $t \rightarrow \infty$, the variance decays to zero and $\bar{C}_t \rightarrow \bar{c}$, where

$$\bar{c} = \min_s \left(\frac{1}{s} E\{\ln[\Lambda_0 M_0(s)]\} \right). \quad (22)$$

The estimate of population growth rate for broom in Discovery Park between 1994 and 1995⁽²⁰⁾ ($\lambda_{1994} = 1.0842$) is lower than the 1993–1994 estimate ($\lambda_{1993} = 1.2167$). Fig. 6 shows the results of including this temporal variability in the model. In these simulations, we used the same dispersal kernel (k_c , Fig. 4E) every year and selected the growth rate Λ_t at random from the set $\{\lambda_{1993}, \lambda_{1994}\}$. The projected average asymptotic speed \bar{c} is 1.13 m/yr: 16% slower than projected under constant 1993–1994 conditions and 36% faster than under constant 1994–1995 conditions.

While the speed of each realization eventually converges to \bar{c} , it should be noted that the spatial extent of a realized invasion would not, in general, converge to $\bar{c}t$. In fact, for large t , $\mathcal{X}_t \approx t\bar{C}_t$, so

$$\text{Var}[\mathcal{X}_t] = t^2 \text{Var}[\bar{C}_t] = t \text{Var} \left\{ \frac{\ln[\Lambda_0 M_0(s^*)]}{s^*} \right\}. \quad (23)$$

Thus the variance in extent grows linearly with time.

3.5. Stage-Structured Models

3.5.1. Formulation

While the IDE of Equation (5) permits a wider range of dispersal distributions than does its reaction-diffusion counterpart of Equation (1), it still treats all individuals within the population as identical. In fact, vital rates and dispersal abilities of individuals often vary dramatically with life history stage. Consider the life cycle of broom⁽²⁰⁾ (Fig. 7). For this species, only adult stages reproduce and only seeds disperse. The seed production of the largest plants is 300 times

higher than that of small reproductive plants, and the mortality rates of seedlings are much higher than those of adults.

Lui⁽⁴⁴⁾ and Neubert and Caswell⁽⁴⁵⁾ show how to incorporate this stage structure into IDE models and how to calculate spread rates. We briefly review their results here. To begin, we must first expand Equation (5) to a system of m difference equations (one equation for each of the m stages). Designating n_i as the population density in the i th stage and b_{ij} as the per-capita production of stage i individuals at time $t + 1$ by stage j individuals at time t , we have

$$n_i(y, t + 1) = \sum_{j=1}^m b_{ij}(n_1(y, t), \dots, n_m(y, t))n_j(y, t), \quad (24)$$

for $i = 1, \dots, m$, or in the more familiar matrix notation,

$$\mathbf{n}(y, t + 1) = \mathbf{B}_n \mathbf{n}(y, t), \quad (25)$$

where \mathbf{B}_n is the density-dependent population projection matrix. (We assume that density dependence acts in the same way at every location.)

To allow for stage-specific dispersal, we must specify a dispersal kernel for each of the m^2 possible transitions between stages. We define $k_{ij}(x, y)$ to be the probability that an individual making the transition from stage j to stage i moves from location y to location x . If there is no dispersal during a given transition, the associated kernel is the Dirac delta function.

The stage-structured analog of Equation (6) is then given as follows:

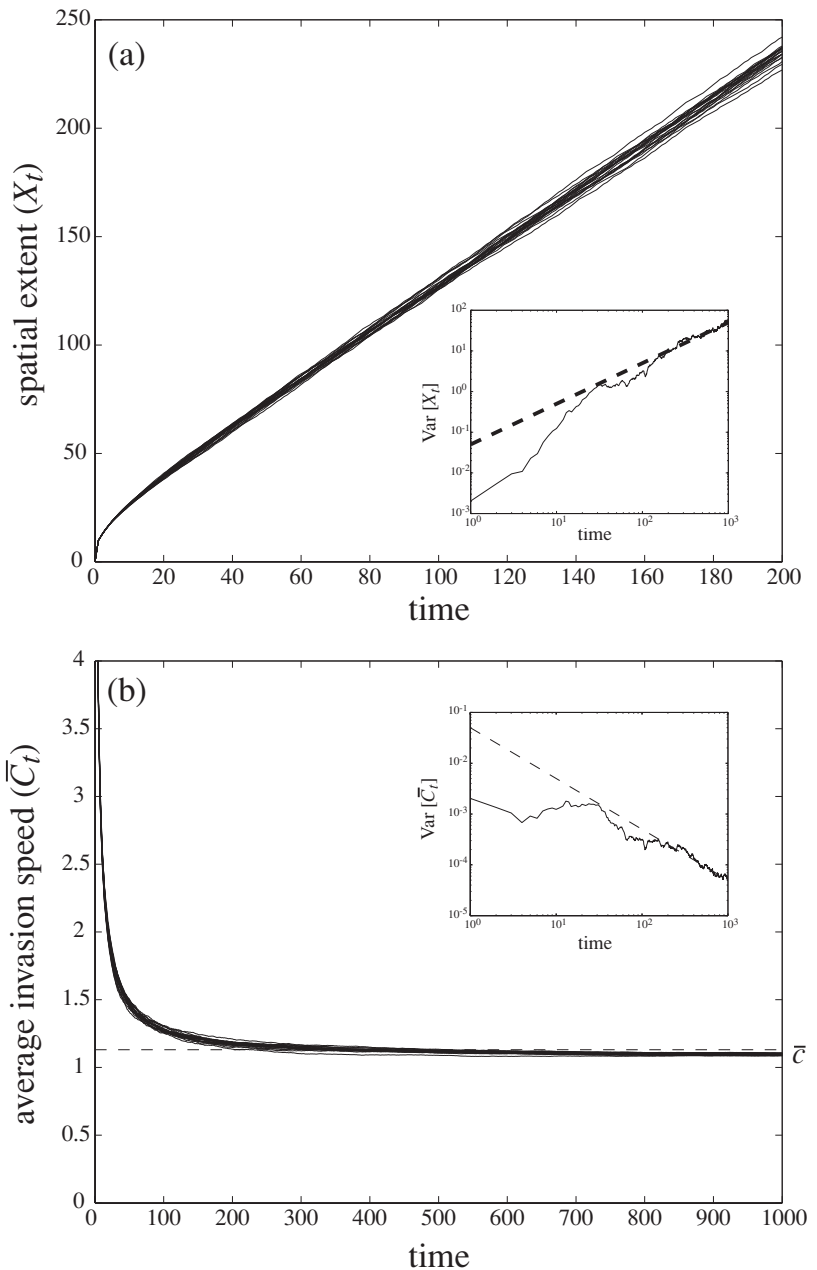
$$n_i(x, t + 1) = \int_{-\infty}^{\infty} \sum_{j=1}^m k_{ij}(x - y) b_{ij}(n_1(y, t), \dots, n_m(y, t)) n_j(y, t) dy, \quad (26)$$

for $i = 1, \dots, m$. Just as the notation of Equation (24) is simplified by Equation (25), if we create the matrix $\mathbf{K}(x - y)$ from the kernels $k_{ij}(x - y)$, the complex notation of Equation (26) is simplified to

$$\mathbf{n}(x, t + 1) = \int_{-\infty}^{\infty} [\mathbf{K}(x - y) \circ \mathbf{B}_n] \mathbf{n}(y, t) dy. \quad (27)$$

The symbol “ \circ ” stands for the Hadamard product,⁽⁴⁶⁾ whereby matrices are multiplied element-wise. (That is, the element in the i th row and j th column of $\mathbf{K}(x - y) \circ \mathbf{B}_n$ is $k_{ij}(x - y) b_{ij}(y)$.)

Fig. 6. Invasion dynamics in a stochastic environment. Using the composite ant/ballistic dispersal kernel with $p = 1$ (Fig. 4E), we simulated 20 realizations of Equation (19) by choosing λ at random between $\lambda_{1993} = 1.2167$ and $\lambda_{1994} = 1.0842$ at each time step. (a) Extent (X_t) of each realization as a function of time. The variance in extent, over the ensemble of realizations, grows linearly with time (inset). For each realization, the average invasion speed converges to the constant \bar{c} as predicted by Equation (22), and the ensemble variance grows like t (inset).



3.5.2. Stage-Structured Invasion Dynamics

As long as the matrices \mathbf{K} and \mathbf{B}_n meet certain biologically reasonable technical assumptions,^(44,45) and there are no Allee effects, then all populations governed by Equation (27) that start in a confined area converge to a traveling wave solution with speed given by

$$c = \min_{s>0} \left[\frac{1}{s} \ln \rho_1(s) \right]. \tag{28}$$

In Equation (28), $\rho_1(s)$ is the largest eigenvalue of the matrix $\mathbf{M}(s) \circ \mathbf{B}_0$, the elements of the matrix $\mathbf{M}(s)$ are the moment-generating functions of the elements of $\mathbf{K}(x)$, and the matrix \mathbf{B}_0 is the matrix \mathbf{B}_n evaluated at low population densities ($\mathbf{n} \approx 0$).

The life cycle graph for broom is shown in Fig. 7. Dashed lines indicate transitions during which dispersal occurs. There are seven stages: seeds, seedlings (one-year olds), juveniles, and four size classes of adults. The projection interval is one year, with a

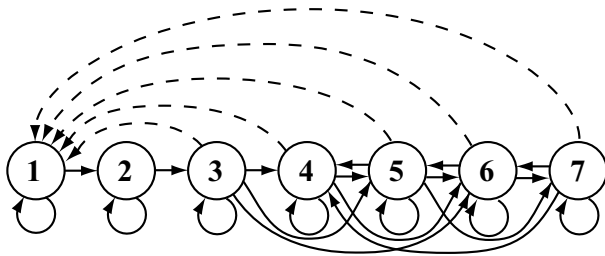


Fig. 7. Life cycle graph for broom (*Cytisus scoparius*). Stages are numbered as follows: (1) seeds, (2) seedlings, (3) juveniles, (4) small adults (<100 g), (5) medium adults (100–400 g), (6) large adults (400–900 g), and (7) extra-large adults (>900 g). Dashed arrows represent transitions during which there is dispersal.

census performed at the end of the dry season, after all seeds have matured. Parker⁽²⁰⁾ estimated the demographic matrix \mathbf{B}_0 in Discovery Park, at the leading edge of an invasion front, over the 1993–1994 and 1994–1995 seasons. It is from these matrices that we calculated the population growth rates used in the unstructured models above. We will use the 1993–1994 matrix for our illustration here

$$\mathbf{A} = \mathbf{B}_0 = \begin{pmatrix} 0.741 & 0 & 3.4 & 47.1 & 108.7 & 1120 & 3339 \\ 0.00105 & 0.31 & 0 & 0 & 0 & 0 & 0 \\ 0 & 0.35 & 0.31 & 0.024 & 0 & 0 & 0 \\ 0 & 0.038 & 0.29 & 0.39 & 0 & 0 & 0 \\ 0 & 0 & 0.069 & 0.44 & 0.32 & 0 & 0.091 \\ 0 & 0 & 0 & 0 & 0.44 & 0.53 & 0.091 \\ 0 & 0 & 0 & 0 & 0.029 & 0.4 & 0.73 \end{pmatrix}. \tag{29}$$

If seed dispersal is independent of plant size (there is no evidence in our data to suggest otherwise⁽³⁹⁾), the matrix of dispersal kernels for broom is the 7×7 matrix

$$\mathbf{K}(x) = \begin{pmatrix} \delta(x) & k_c(x) & k_c(x) & k_c(x) & k_c(x) & k_c(x) & k_c(x) \\ \delta(x) & \delta(x) & \delta(x) & \delta(x) & \delta(x) & \delta(x) & \delta(x) \\ \vdots & \vdots & \vdots & \vdots & \vdots & \vdots & \vdots \\ \delta(x) & \delta(x) & \delta(x) & \delta(x) & \delta(x) & \delta(x) & \delta(x) \end{pmatrix}, \tag{30}$$

and the matrix of moment-generating functions for broom is given by

$$\mathbf{M}(s) = \begin{pmatrix} 1 & M_c(s) & M_c(s) & M_c(s) & M_c(s) & M_c(s) & M_c(s) \\ 1 & 1 & 1 & 1 & 1 & 1 & 1 \\ \vdots & \vdots & \vdots & \vdots & \vdots & \vdots & \vdots \\ 1 & 1 & 1 & 1 & 1 & 1 & 1 \end{pmatrix}. \tag{31}$$

Note that while seedlings produce no seed ($a_{12} = 0$) we include the possibility of dispersal during the transition from seedling to seed ($k_{12}(x) = k_c(x)$, $m_{12}(s) = M_c(s)$) because if seedlings did produce

seeds we assume that they would disperse like all the rest.

In Fig. 8 we show the result of simulating Equation (27). In order to prevent the population at any location from growing without bound, we introduced negative density dependence in the transitions from seedlings to juvenile and adult stages of the form

$$b_{j2}(\mathbf{n}(t, y)) = a_{j2} \exp \left[- \sum_{i=4}^7 n_i(y, t) \right] \quad \text{for } 3 \leq j \leq 7. \tag{32}$$

This form of density dependence is consistent with the observation that very few seedlings mature when surrounded by adult plants.⁽²⁰⁾ We assumed that all other transitions were density independent and given by their entries in \mathbf{A} .

The pattern of invasion shown in Fig. 8 is typical. The population density in each stage forms a traveling wave and, asymptotically, each wave moves with the same speed (given by Equation (28)) of $c \approx 0.46$ m/yr. This speed is 66% less than the projection based on the unstructured Equation (6).

It is a straightforward exercise to show that, all else being equal, invasion rate projections based on unstructured models overestimate actual invasion rates compared with projections from structured models.⁽⁴⁵⁾ This is because unstructured models ignore the fact that some transitions do not involve dispersal. But reducing this bias is only one of the advantages of including stage structure. More importantly, stage-structured models link invasion rates to processes that occur within the life cycle of an individual. It is these processes that can be changed by management tactics, manipulated in experiments, or altered by changes in the environment. Thus stage-structured models are more useful than unstructured models, as well as potentially more accurate.

3.5.3. Perturbation Analyses

We now present the formulae for the sensitivity and elasticity of invasion rate to changes in the vital rates (i.e., the entries in the matrix \mathbf{A}). There are a number of compelling reasons to carry out such an analysis.^(45,47) For example, the errors in estimating the parameters result in errors in c . The most important errors will be in the parameters to which c is most sensitive. Information on the sensitivity of c can thus be used to design sampling procedures that maximize the precision of the estimates of the most critical parameters. Sensitivity analysis of invasion rates may also be valuable in the evaluation of management strategies for the control of invasive species.⁽⁴⁸⁾

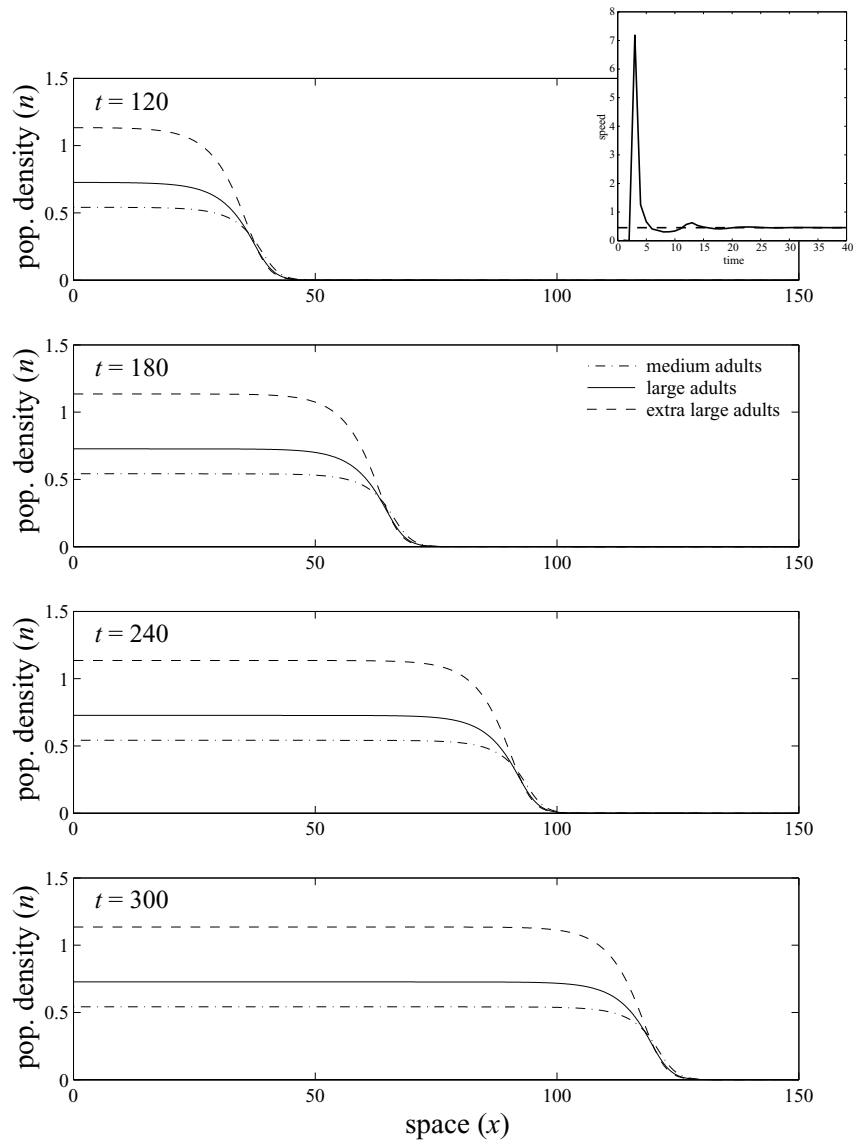


Fig. 8. Dynamics of a stage-structured broom invasion. Equation (27) was iterated 300 times from an initial distribution concentrated at the origin. The elements of the matrix \mathbf{B}_n were given by the corresponding elements in the matrix \mathbf{A} as given in Equation (29), except that $b_{j2}(\mathbf{n}(t, y))$ is given by Equation (32) to account for density dependence. As $t \rightarrow \infty$, the instantaneous speed converges to 0.46 m/yr, the value predicted by Equation (28) (inset).

The matrix

$$\frac{\partial c}{\partial a_{ij}} = \frac{m_{ij}(s^*)}{s^* \rho_1(s^*)} \frac{v_i w_j}{\langle \mathbf{v}, \mathbf{w} \rangle} \quad (33)$$

contains the sensitivities of c to changes in the demographic parameters a_{ij} .⁽⁴⁵⁾ The elasticity of c to those same changes is given by

$$\frac{a_{ij}}{c} \frac{\partial c}{\partial a_{ij}}. \quad (34)$$

In these formulae, the vectors \mathbf{v} and \mathbf{w} are the dominant left and right eigenvectors of the matrix $\mathbf{B}_0 \circ \mathbf{M}(s^*)$, s^* is the value of s that produces the minimum

in the formula for c (Equation (28)), and the operator $\langle \cdot, \cdot \rangle$ is the scalar product.

The sensitivity matrix for broom in Discovery Park (Fig. 9A) shows that invasion rate is most sensitive to changes in the transitions from seeds to large-size class adults. The elasticity matrix (Fig. 9B) shows that the largest proportional changes in invasion rate are generated by changes in the survival of seeds in the seed bank (a_{11}) and the germination rate (a_{21}). The next largest elasticities occur for the transitions from smaller to larger stages and the survival of extra-large adults.

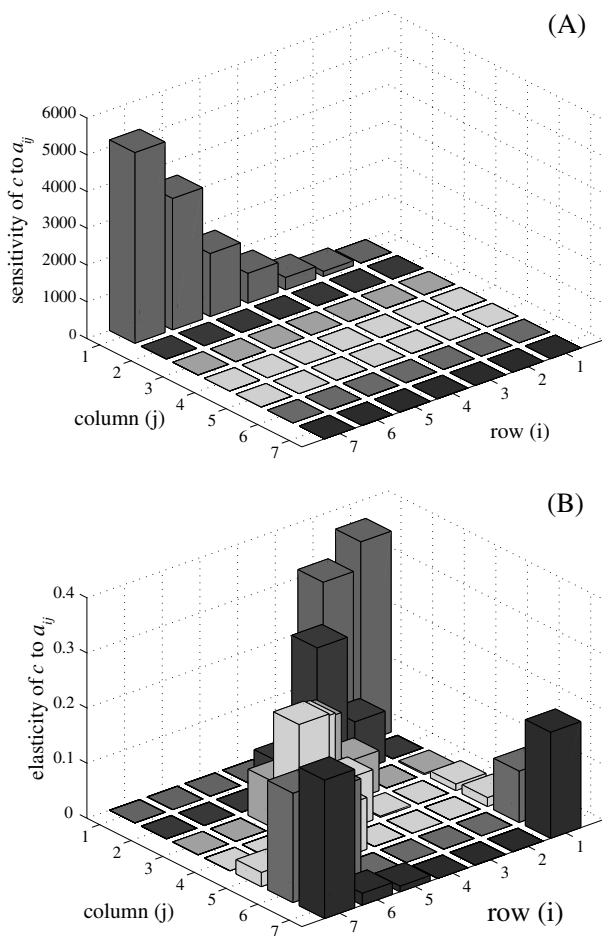


Fig. 9. Matrices of (A) sensitivity and (B) elasticity of invasion rate to demographic parameters, as calculated in Equations (33) and (34), respectively.

4. DISCUSSION

4.1. IDEs and Other Models

IMP models are a convenient way to combine demographic models with models for spatial dispersal. They have several strengths. First, because they are in matrix form, they are particularly well suited for dealing with stage-structured populations, and classification of individuals by stage is often more biologically useful than a classification by age. Second, they are relatively easy to analyze; computation of invasion speed amounts to the calculation of an eigenvalue of a matrix (Equation (28)). Finally, they are particularly easy to connect with data. There are statistical procedures for parameterizing matrix models from many kinds of data,⁽⁴⁷⁾ and dispersal kernels and moment-

generating functions also lend themselves to empirical estimation.^(42,49–51)

There are, of course, alternatives to IDEs for modeling spatial population dynamics. For example, continuous-time models^(52,53) that amount to spatial extensions of Lotka's integral equation have been used to project rates of spread for a variety of plant, animal, and fungal species.⁽⁵⁴⁾ As is often the case in data analysis, the mathematical model one finally chooses is as likely to depend on the tastes and talents of the analyst as it is to depend on the dictates of biology.

4.2. Conservation and Management

Demographic models, and in particular matrix population models, have become influential tools in conservation biology.^(47,55) They are used to help choose among management alternatives by projecting the likely result of various interventions. For conservation questions that involve spatial processes, such as curbing the spread of an invasive species or assessing relative risk, IMP models can be used in the same way.

The objective of nonnative species management is to slow the spread of invading populations, but the management tools at hand usually target particular vital rates of the organism. For example, a biocontrol agent might kill seeds; a prescribed fire might kill adults but increase germination. To meet their objectives, managers must choose among these tools, and they need demographic information to guide their choices. As a result, prospective perturbation analyses (i. e., sensitivity and elasticity analyses) are a useful link between models and management.⁽⁵⁶⁾ When applied sensibly, these analyses help to distinguish the changes to the vital rates that are likely to have a significant impact and thereby help to identify potential management strategies.

A perturbation analysis of invasion rate, as outlined in Section 3.5, should accompany any projection of invasion rate used to guide management. For broom, the perturbation analysis indicates that transitions involving the survival and germination of seeds have the highest elasticities, but these were not vastly larger than the elasticities for other transitions. Broom does not seem to have any particular "Achilles heel" when it comes to invasion speed, a result consistent with previous analyses.⁽²⁰⁾

Because invasion speed is a nonlinear function of the elements of the matrix from which it is derived, and because sensitivity and elasticity analyses

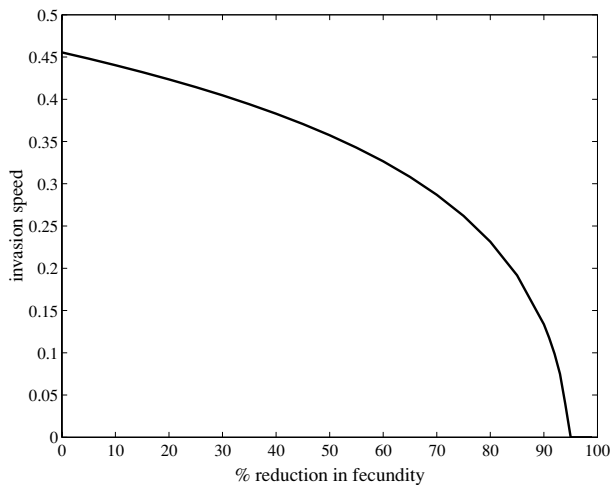


Fig. 10. Reduction in invasion speed that would result from a given reduction in the fecundity of broom (uniformly applied to elements a_{12} through a_{17} in the top row of Matrix (29)).

are based on linear approximations, there is the potential for prognoses based on these approximations to be inaccurate. The danger is largest when perturbations are large. In these cases, it is advisable to compute the change in invasion rate directly from Equation (28). We did this for broom to explore the efficacy of a potential seed predator that would reduce fecundity (elements a_{12} through a_{17}) uniformly across plant size. The result, shown in Fig. 10, is that such a seed predator would have to be extremely effective to stop the spread of broom. Invasion speed drops slowly as fecundity is reduced, until a large fraction of seeds are destroyed. Over 95% of the seeds would have to be destroyed to stop the invasion.

4.3. Scale

Given broom's status as a noxious weed, the projected speed for Discovery Park that we derived from our stage-structured model ($c \approx 0.46$ m/yr) might seem surprisingly slow. The historical record of broom spread in the Pacific Northwest⁽¹⁶⁾ suggests that at the regional scale, this species was able to move quite rapidly into new areas. The discrepancy between historical data and our projected invasion rate, however, does not lie in any failure of the model but rather is explained by a mismatch of scales.

Spread at the regional or continental scale primarily reflects human-mediated long-distance dispersal events. These separate colonization events could be intentional, such as the sharing of nursery stock with

a gardener from a distant county, or unintentional, such as a seed hitchhiking on an interstate shipment of logs. To project spread rates at the regional scale, this long-distance dispersal would need to be quantified and added to the model in the form of a long tail in the dispersal kernel. However, if one used the resulting long-tailed kernel to analyze the spread of broom at the scale of an individual field or preserve, the analysis would be greatly misleading. A 0.5 m/yr spread rate estimated from the expansion of individual stands of broom in Australia⁽⁵⁷⁾ is quite comparable to our projection of local-scale invasion, and suggests that our model captures the important local-scale phenomena. In general, care must be taken to formulate models and estimate their parameters at a scale appropriate to the issue at hand.

ACKNOWLEDGMENTS

We would like to acknowledge support for our work from the National Science Foundation (DMS-9973312, DEB-9527400, DEB-9808501) and from the Working Group on the Synthesis of Demography and Dispersal at the National Center for Ecological Analysis and Synthesis. We would also like to thank Mark Andersen, Mark Powell, the Society for Risk Analysis, the Theoretical Ecology Section of the Ecological Society of America, and the USDA for organizing the workshop that inspired us to write this article. We acknowledge Hal Caswell for stimulating discussions, Woods Hole Oceanographic Institution Contribution 11184.

REFERENCES

1. Wilcove, D. S., Rothstein, D., Dubow, J., *et al.* (1998). Quantifying threats to imperiled species in the United States. *Bio-science*, 48(8), 607–615.
2. U. S. Executive Office. (1999). Executive Order 13112. Invasive species. *Federal Register*, 64, 6183–6186.
3. Pimentel, D., McNair, S., Janecka, J., *et al.* (2001). Economic and environmental threats of alien plant, animal, and microbe invasions. *Agriculture, Ecosystems and Environment*, 84(1), 1–20.
4. Agriculture, Resource Management Council of Australia and New Zealand, and Australia Environment and Conservation Council Forestry Ministers. (1997). *The National Weeds Strategy: A Strategic Approach to Weed Problems of National Significance*. Canberra, Australia: Commonwealth of Australia.
5. Lonsdale, W. M., & Smith, C. S. (2001). Evaluating pest screening procedures—Insights from epidemiology and ecology. In R. H. Groves, F. D. Panetta, & J. G. Virtue, (Eds.), *Weed Risk Assessment*. Collingwood, Australia: CSIRO Publishing.
6. Smith, C. S., Lonsdale, W. M., & Fortune, J. (1999). When to ignore advice: Invasion predictions and decision theory. *Biological Invasions*, 1(1), 89–96.

7. Randall, J. M. (1996). Assessment of the invasive weed problem on preserves across the United States. *Endangered Species Update*, 12, 4–6.
8. Hiebert, R. D. (1997). Prioritizing invasive plants and planning for management. In J. O. Luken & J. W. Theuret (Eds.), *Assessment and Management of Plant Invasions* (pp. 195–212). New York: Springer-Verlag.
9. Parker, I. M., Simberloff, D., Lonsdale, W. M., et al. (1999). Impact: Toward a framework for understanding the ecological effects of invaders. *Biological Invasions*, 1(1), 3–19.
10. Zavaleta, E. (2000). Valuing ecosystem services lost to Tamarix invasion in the United States. In H. A. Mooney & R. J. Hobbs (Eds.), *Invasive Species in a Changing World* (pp. 261–300). Washington, DC: Island Press.
11. Kot, M., & Schaffer, M. W. (1986). Discrete-time growth-dispersal models. *Mathematical Biosciences*, 80, 109–136.
12. Kot, M. (in press). Do invading organisms do the wave? *Canadian Quarterly of Applied Mathematics*.
13. Hosking, J. R., Smith, J. M. B., & Sheppard, A. W. (1996). The biology Australian weeds: 28. *Cytisus scoparius* (L) link subsp. *scoparius*. *Plant Protection Quarterly*, 11(3), 102–108.
14. Paynter, Q. S., Fowler, S. V., Memmott, J., et al. (1998). Factors affecting the establishment of *Cytisus scoparius* in southern France: Implications for managing both native and exotic populations. *Journal of Applied Ecology*, 35, 582–595.
15. Luken, J. O., & Thieret, J. W. (1997). *Assessment and Management of Plant Invasions*. New York: Springer-Verlag.
16. Isaacson, D. L. (2000). Impacts of broom (*Cytisus scoparius*) in western North America. *Plant Protection Quarterly*, 15(4), 145–148.
17. Smith, J. M. B. (1994). The changing ecological impact of broom (*Cytisus scoparius*) at Barrington Tops, New South Wales. *Plant Protection Quarterly*, 9, 6–11.
18. Parker, I. M., & Reichard, S. H. (1997). Critical issues in invasion biology for conservation science. In P. Fiedler & P. Kareiva (Eds.), *Conservation Biology*. New York: Chapman and Hall.
19. Haubensak, K. A., & Parker, I. M. (in press). Soil changes accompanying invasion of the exotic shrub *Cytisus scoparius* in glacial outwash prairies of western Washington (USA). *Plant Ecology*.
20. Parker, I. M. (2000). Invasion dynamics of *Cytisus scoparius*: A matrix model approach. *Ecological Applications*, 10, 726–743.
21. Bossard, C. C. (1990). Tracing of ant-dispersed seeds: A new technique. *Ecology*, 71(6), 2370–2371.
22. Hotelling, H. (1921). *A Mathematical Theory of Migration*. Master's thesis, University of Washington.
23. Hotelling, H. (1978). A mathematical theory of migration. *Environment and Planning A*, 10, 1223–1239.
24. Fisher, R. A. (1937). The wave of advance of advantageous genes. *Annals of Eugenics*, 7, 353–369.
25. Kolmogorov, A. N., Petrowsky, N., & Piscounov, N. S. (1937). Étude de l'équations de la diffusion avec croissance de la quantité de matière et son application a un problème biologique. *Moscow University Bulletin of Mathematics*, 1, 1–25.
26. Aronson, D. G., & Weinberger, H. F. (1975). Nonlinear diffusion in population genetics, combustion, and nerve propagation. In J. Goldstein (Ed.), *Partial Differential Equations and Related Topics*, Vol. 446 (pp. 5–49). Berlin, Germany: Springer-Verlag.
27. Andow, D. A., Kareiva, P. M., Levin, S. A., et al. (1990). Spread of invading organisms. *Landscape Ecology*, 4, 177–188.
28. Shigesada, N., & Kawasaki, K. (1997). *Biological Invasions: Theory and Practice*. Oxford, UK: Oxford University Press.
29. Okubo, A. (1980). *Diffusion and Ecological Problems: Mathematical Models*. New York: Springer-Verlag.
30. Andersen, M. (1991). Properties of some density-dependent integrodifference equation population models. *Mathematical Biosciences*, 104, 135–157.
31. Kot, M., Lewis, M. A., & van den Driessche, P. (1996). Dispersal data and the spread of invading organisms. *Ecology*, 77, 2027–2042.
32. Kot, M. (1992). Discrete-time travelling waves: Ecological examples. *Journal of Mathematical Biology*, 30, 413–436.
33. Weinberger, H. F. (1978). Asymptotic behavior of a model of population genetics. In J. Chadam (Ed.), *Nonlinear Partial Differential Equations and Applications*, Vol. 684 (pp. 47–96). Berlin, Germany: Springer-Verlag.
34. Weinberger, H. F. (1982). Long-time behavior of a class of biological models. *SIAM Journal of Mathematical Analysis*, 13, 353–396.
35. Neubert, M. G., Kot, M., & Lewis, M. A. (1995). Dispersal and pattern formation in a discrete-time predator-prey model. *Theoretical Population Biology*, 48(1), 7–43.
36. Beer, T., & Swain, M. D. (1977). On the theory of explosively dispersed seeds. *New Phytologist*, 78, 681–694.
37. Broadbent, S. R., & Kendall, D. G. (1953). The random walk of *trichostrongylus retortaeformis*. *Biometrika*, 9, 460–465.
38. Lewis, M. A., Neubert, M. G., Clark, J., et al. (in preparation). A guide to the construction and interpretation of 1-d integrodifference equation models for biological invasions.
39. Parker, I. M. (1996). *Ecological Factors Affecting Rates of Population Growth and Spread in Cytisus scoparius, an Invasive Exotic Shrub*. PhD thesis, University of Washington.
40. Bracewell, R. N. (1986). *The Fourier Transform and Its Applications*, 2nd ed. New York: McGraw-Hill.
41. Abramowitz, M., & Stegun, I. A. (1965). *Handbook of Mathematical Functions with Formulas, Graphs, and Mathematical Tables*. Washington, DC: U.S. Government Printing Office.
42. Clark, J., Horvath, L., & Lewis, M. A. (2001). On the estimation of spread rate for a biological population. *Statistics and Probability Letters*, 51, 225–234.
43. Neubert, M. G., Kot, M., & Lewis, M. A. (2000). Invasion speeds in fluctuating environments. *Proceedings of the Royal Society of London, Series B: Biological Sciences*, 267(1453), 1603–1610.
44. Lui, R. (1989). Biological growth and spread modeled by systems of recursions. I. Mathematical theory. *Mathematical Biosciences*, 93, 269–295.
45. Neubert, M. G., & Caswell, H. (2000). Demography and dispersal: Calculation and sensitivity analysis of invasion speed for structured populations. *Ecology*, 81(6), 1613–1628.
46. Horn, R. A., & Johnson, C. R. (1985). *Matrix Analysis*. Cambridge, UK: Cambridge University Press.
47. Caswell, H. (2001). *Matrix Population Models: Construction, Analysis, and Interpretation*, 2nd ed. Sunderland, MA: Sinauer Associates.
48. Sharov, A. A., & Liebhold, A. M. (1998). Bioeconomics of managing the spread of exotic pest species with barrier zones. *Ecological Applications*, 8(3), 833–845.
49. Silverman, B. W. (1986). *Density Estimation for Statistics and Data Analysis*. London, UK: Chapman and Hall.
50. Härdle, W. (1990). *Applied Nonparametric Regression*. Cambridge, UK: Cambridge University Press.
51. de Wit, T. D., & Floriani, E. (1998). Estimating probability densities from short samples: A parametric maximum likelihood approach. *Physical Review E*, 58, 5115–5122.
52. Van den Bosch, F., Metz, J. A. J., & Diekmann, O. (1990). The velocity of spatial population expansion. *Journal of Mathematical Biology*, 28, 529–565.
53. Diekmann, O., Gyllenberg, M., Metz, J. A. J., et al. (1998). On the formulation and analysis of general deterministic

- structured population models. I. Linear theory. *Journal of Mathematical Biology*, 36, 349–388.
54. Hengeveld, R. (1994). Small-step invasion research. *Trends in Ecology and Evolution*, 9, 339–342.
55. Morris, W. F., & Doak, D. F. (2002). *Quantitative Conservation Biology: Theory and Practice of Population Viability Analysis*. Sunderland, MA: Sinauer.
56. Caswell, H. (2000). Prospective and retrospective perturbation analyses and their use in conservation biology. *Ecology*, 81, 619–627.
57. Downey, P. O., & Smith, J. M. B. (2000). Demography of the invasive shrub scotch broom (*Cytisus scoparius*) at Barrington Tops, New South Wales: Insights for management. *Austral Ecology*, 25, 477–485.